Supplementary Figure S1. Binding of rPMT to lipid extracts from Vero cells. Lipid extracts from Vero cells were developed on TLC plates with ternary solvent systems of chloroform/methanol/0.05M $CaCl_2$ at the indicated ratios. The TLC plates were then blocked with BSA and overlayed with ^{125}I-rPMT, as described in the experimental section. I, phosphorimage of ^{125}I-rPMT. C, $CuSO_4$-stained image after recording the autoradiogram. Bands A, B, C are three major lipid components showing affinity for rPMT.

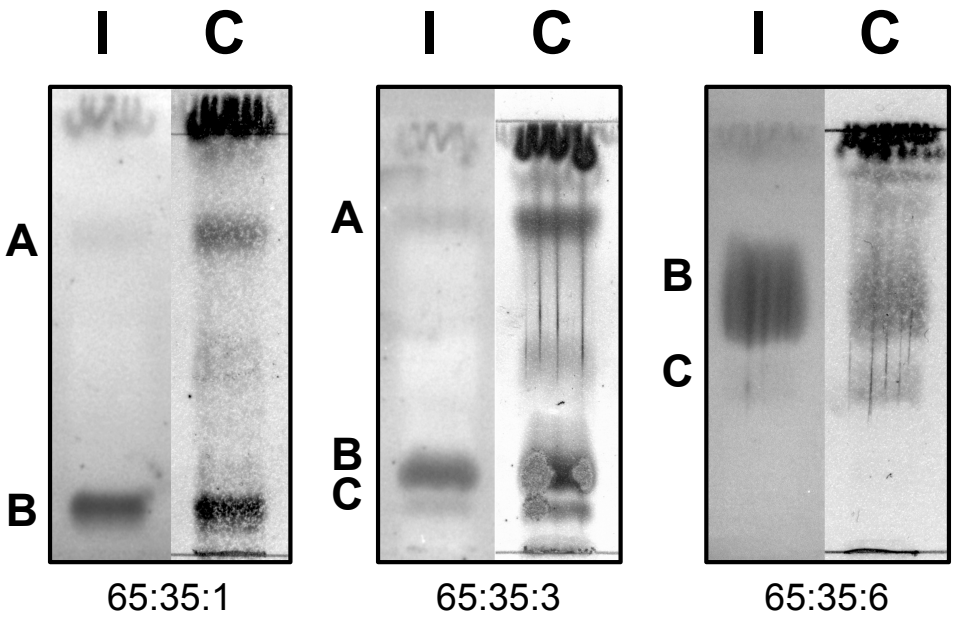

Supplementary Figure S2. Binding of rPMT to gangliosides. Triple replicas of TLC plates loaded with: lane 1, GM1 (50 µg); lane 2, GM2 (50 µg); lane 3, GM3 (bottom band) plus two forms of Lac-Cer (upper bands) (50 µg each); and lane 4, bovine brain gangliosides (50 µg). The plates were developed in solvent system 65:30:1.5 (v/v/v, chloroform/methanol/0.05% $CaCl_2$). Left: image of Orcinol-stained TLC plate; Middle: autoradiogram after incubation with ^{125}I-rPMT at 4°C for 16 hr; Right: autoradiogram after incubation with ^{125}I-rPMT at 37°C for 1 hr.

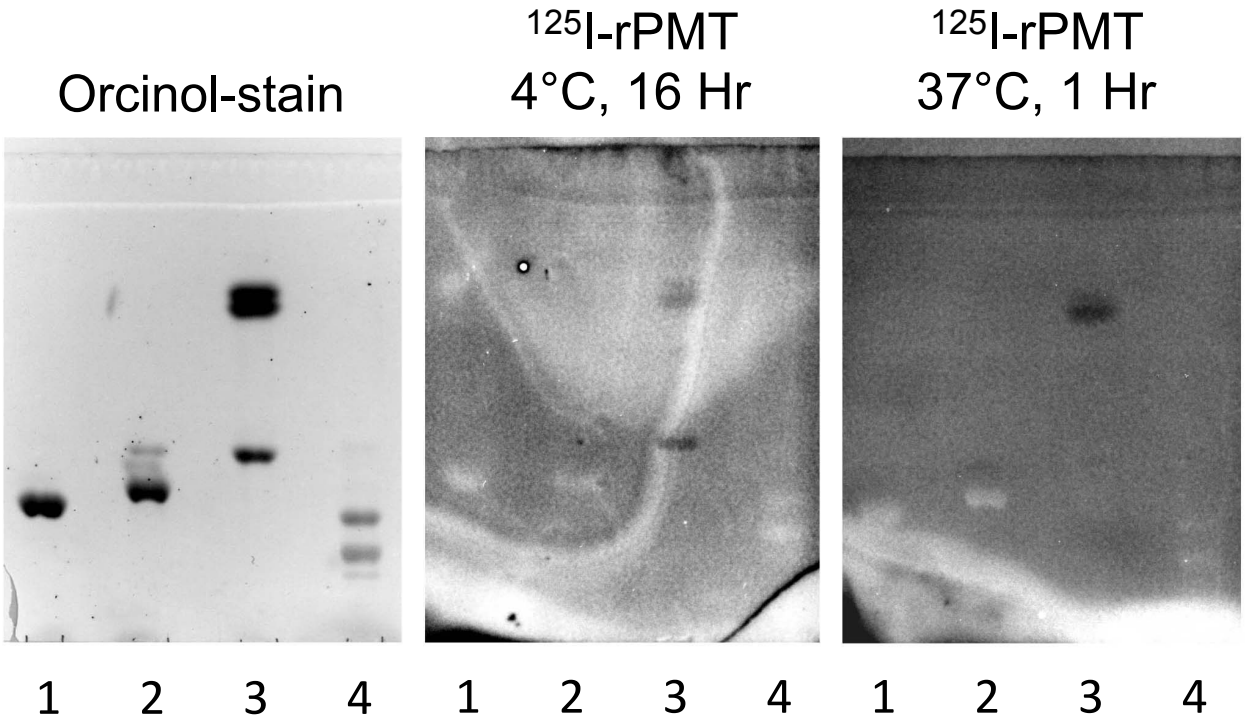

Supplementary Figure S3. Binding of PMT and PMT fragments to nonpolar lipid components. Stearic acid (SA), 1-stearoyl-*rac*-glycerol (MG), 1,2-distearoyl-rac-glycerol (DG) and cholesterol (CHL) (20 µg each) were loaded on the TLC plate and developed in a solvent system of 94:6 (v/v, chloroform/methanol), as described in the experimental section. Left: image of $CuSO_4$-stained TLC plate; Right: autoradiogram after incubation with ^{125}I-rPMT.

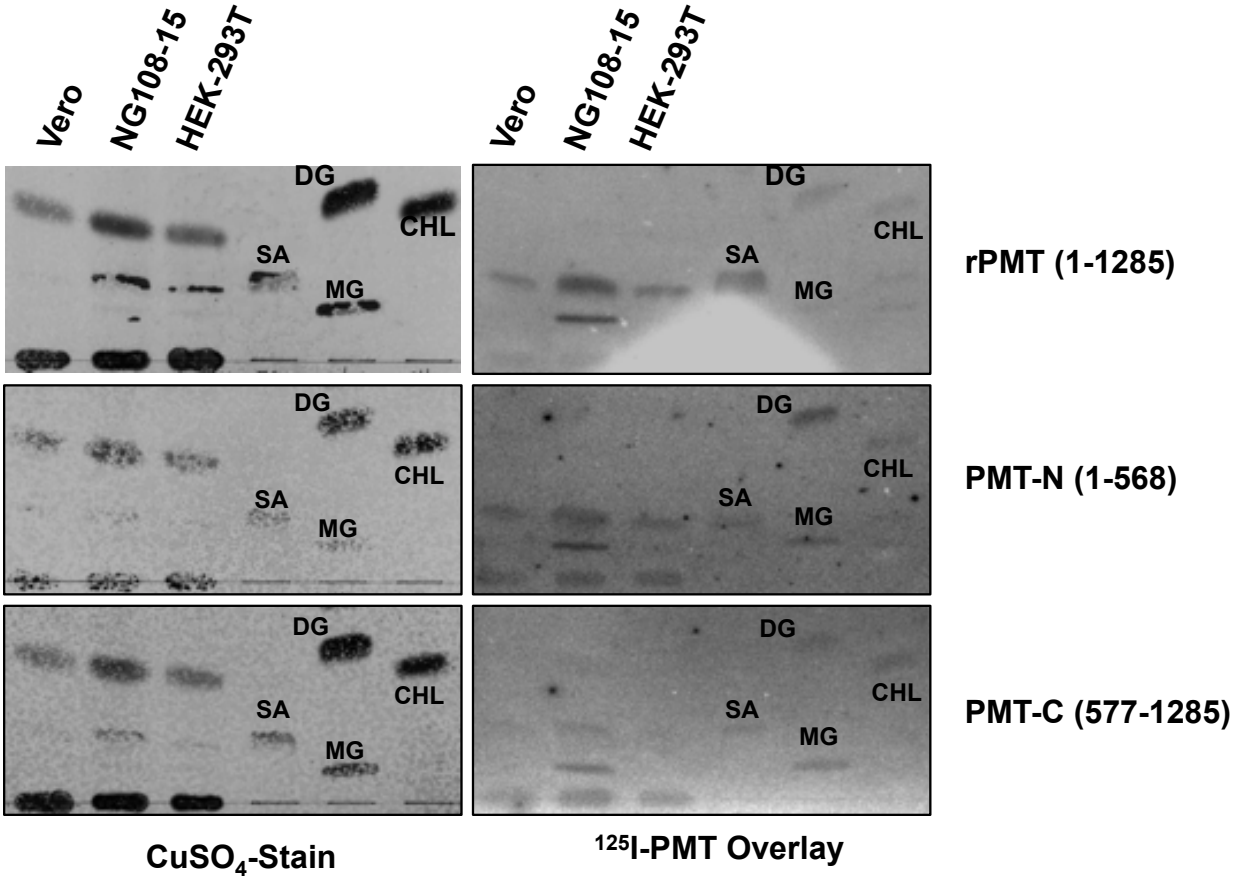

Supplementary Figure S4. Binding of PMT and PMT fragments to less polar ceramides. Ceramide I (CerI), ceramide II (CerII), glucosylceramide (GlcC), galactosylceramide (GalC) and lactosylceramide (LacC) (20µg each) were loaded on the TLC plate and developed in a solvent system of 85:15:1 (v/v/v, chloroform/methanol/0.05% $CaCl_2$), as described in the experimental section. Left: image of $CuSO_4$-stained TLC plate; Right: autoradiogram after incubation with ^{125}I-rPMT.

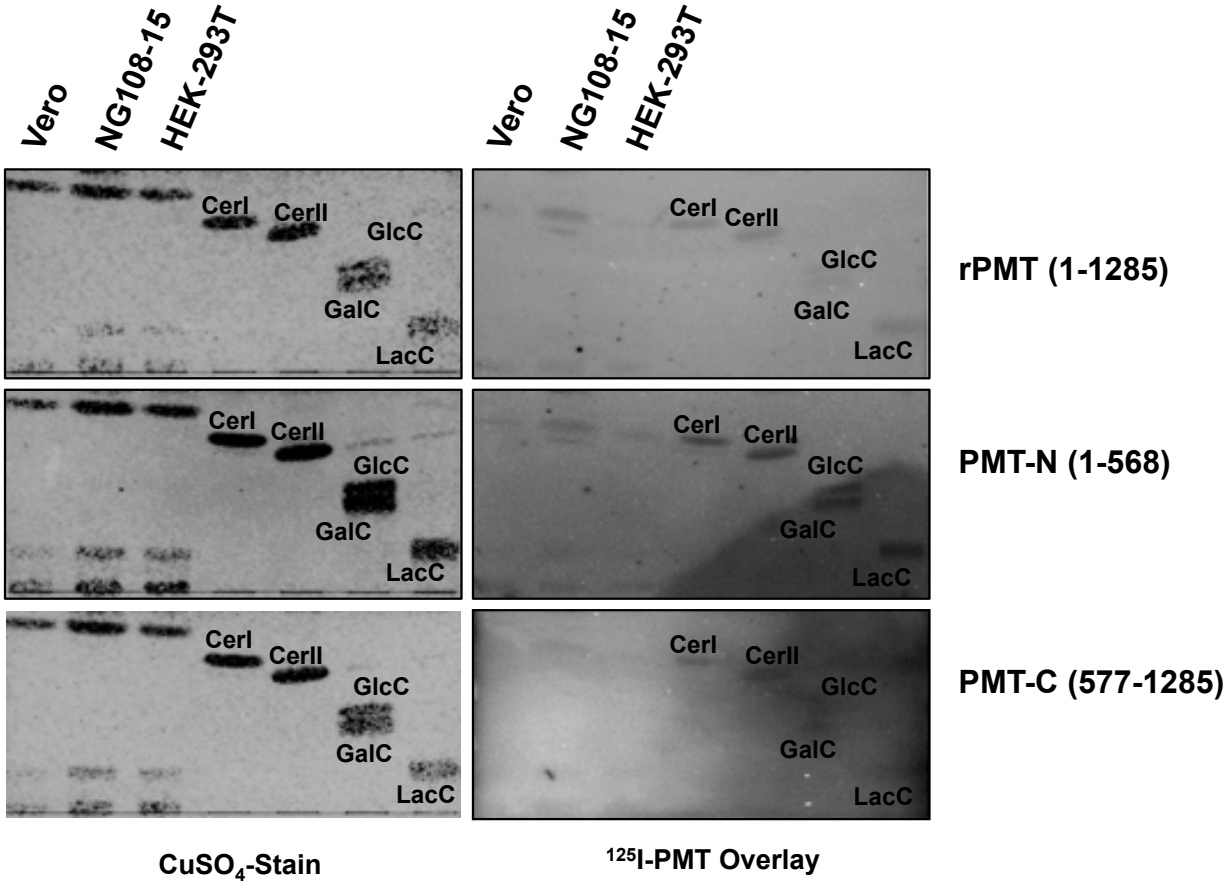

Supplementary Figure S5. SPR of PMT-N binding to reconstituted phospholipid vesicles on an L1 chip. Sensorgrams generated with PMT-N binding to vesicles of phospholipids, PC only, PC/PS, or PC/SM (as shown in Figure 6), were fitted to a two-component bi-phasic exponential binding model. The kinetic parameters calculated from a least-squares method were used to construct the theoretical curves for total binding and components corresponding to the rapid component and the slow component.

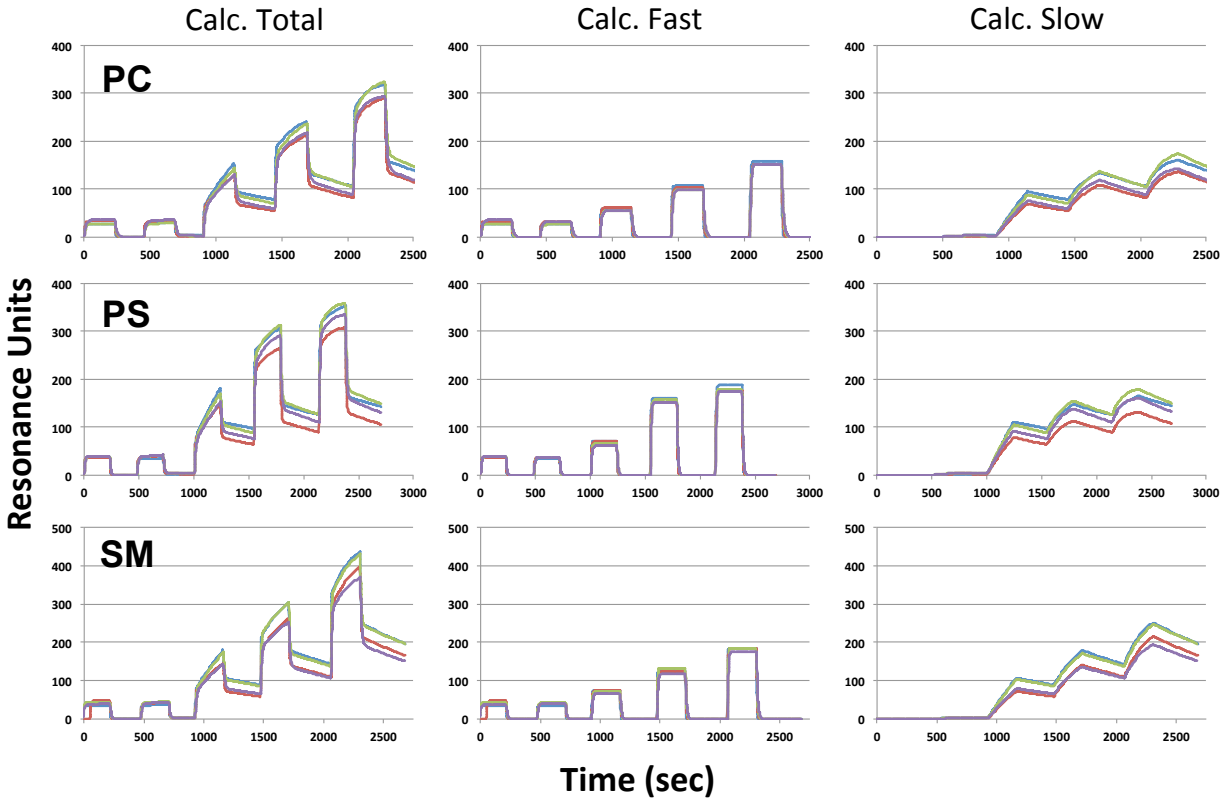

Supplementary Figure S6. SPR sensorgrams of PMT-N binding to cell membranes. SPR sensorgrams of PMT-N binding to membrane ghosts of HEK-293T cells on an L1 chip (left) and the calculated curves, generated according to a rapid-and-slow two-component binding model (middle) or a single-component binding model (right).

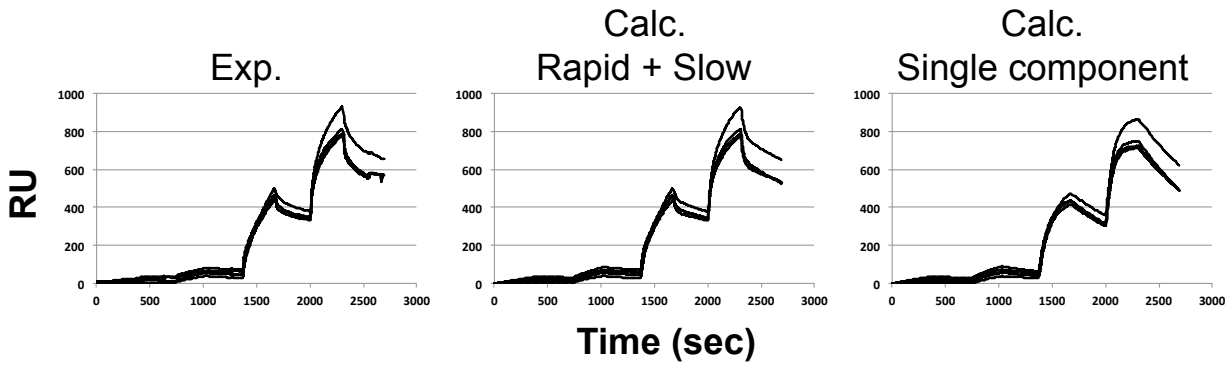

Supplementary Figure S7. Uptake of radiolabeled PMT into Swiss 3T3 cells. To confirm the functional viability of radiolabeled rPMT to bind to and enter cells and traffic to endosomes, Swiss 3T3 cells were incubated with ^{125}I-rPMT at 4°C for 30 min, and then incubated at 37°C for 4 hrs. Cells were harvested and centrifuged to separate pellet (P), containing nucleus, plasma membrane and cellular debris, from cell-free extract supernatant (S), containing cytosol and vesicles. The S fraction was further separated by Opti-prep density gradient centrifugation into 12 fractions (1 mL each). Samples of each fraction collected from the top (fraction #1, low density) to the bottom (fraction #12, high density) were separated by SDS-PAGE. Top panel: phosphorimage of SDS-PAGE gel, showing subcellular localization of radiolabeled PMT. Bottom panel: Western blot of a control SDS-PAGE gel, showing subcellular localization of the endosomal marker EEA1.

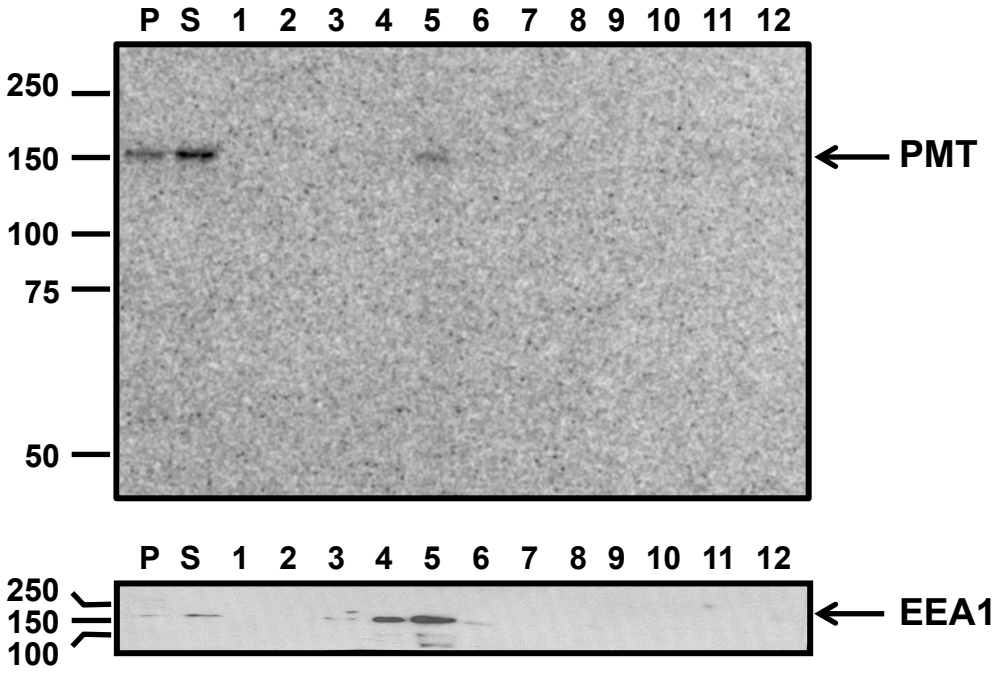

Supplementary Figure S8. Competition between ^{125}I-labeled and unlabeled PMT-N for binding to PC and SM in TLC-overlay assay. ^{125}I-PMT-N(1-568), 100 µg in 10 ml of PBS, was divided in half, and 5 mL of PBS with (lower panels) or without (upper panels) 2 mg of unlabeled PMT-N(1-568) protein was added. These two solutions were used for TLC-overlay experiment with similarly prepared TLC plates loaded with lipid extract from HEK293 cells, PC (50 µg) and SM (50 µg) and developed in a solvent system of 70:30:3 (v/v/v, chloroform/methanol/0.2% $CaCl_2$). Autoradiographs (right panels) were recorded simultaneously using a phosphoimager before visualization with $CuSO_4$ (left panels), as described in the experimental section.

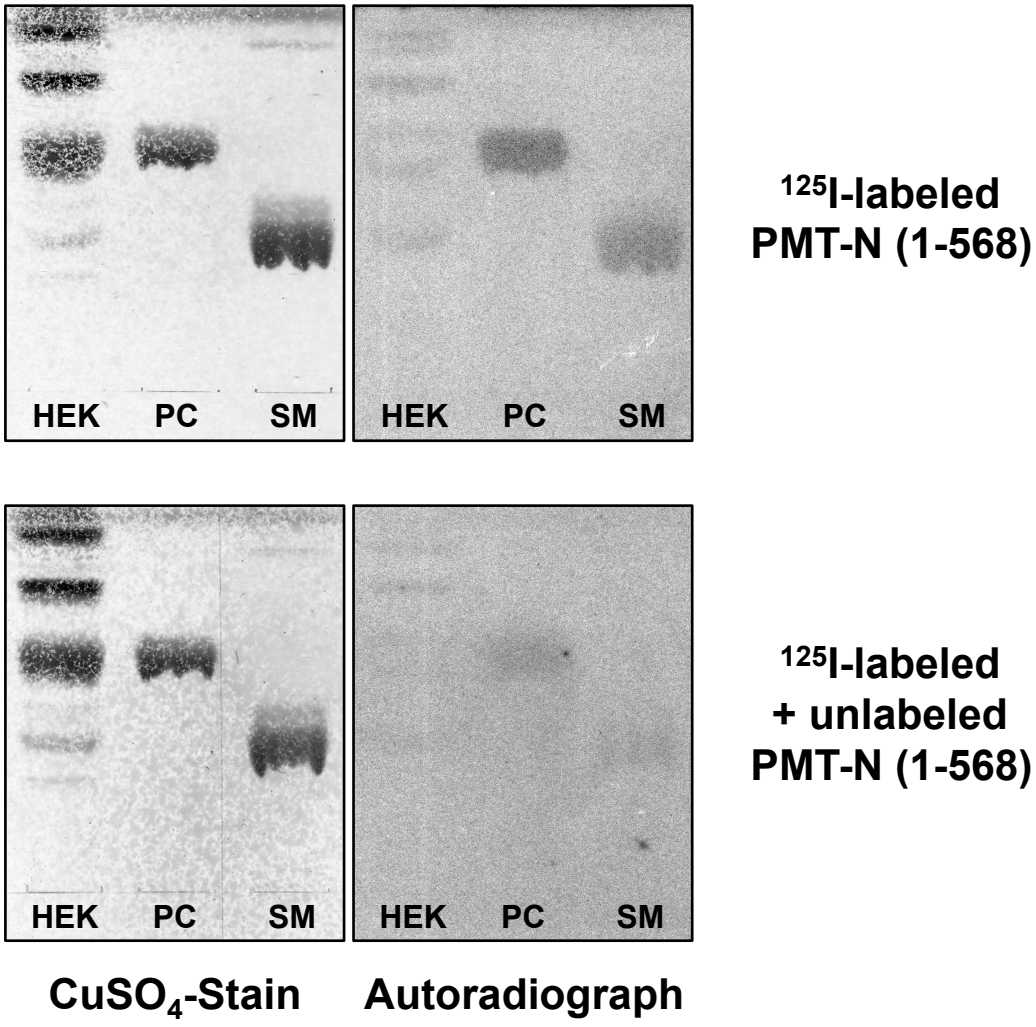

Supplementary Table S1. P values for comparing PMT-N binding to reconstituted membranes. Shown are P values calculated with the t-distribution for comparing PMT-N binding characteristics on reconstituted lipids. The degree of freedom used for *p* value calculation was based on the number of sets (N) with four traces for Rapid B_{max} and Rapid K_D, and the total number of traces (N x 4) for others.

Rapid B_{max}

	PC only	PC/PS	PC/SM
PC only		**0.0034**	**0.0021**
PC/PS	**0.0034**		**0.0018**
PC/SM	**0.0021**	**0.0018**	

Rapid K_D

	PC only	PC/PS	PC/SM
PC only		**0.0010**	**0.0024**
PC/PS	**0.0010**		**0.0039**
PC/SM	**0.0024**	**0.0039**	

Rapid k_{off}

	PC only	PC/PS	PC/SM
PC only		0.5406	0.7226
PC/PS	0.5406		0.7324
PC/SM	0.7226	0.7324	

Slow B_{max}

	PC only	PC/PS	PC/SM
PC only		0.11670	**0.00001**
PC/PS	0.11670		**0.00013**
PC/SM	**0.00001**	**0.00013**	

Slow K_D

	PC only	PC/PS	PC/SM
PC only		0.02501	**0.00031**
PC/PS	0.02501		**0.00001**
PC/SM	**0.00031**	**0.00001**	

Slow k_{off}

	PC only	PC/PS	PC/SM
PC only		**0.00456**	**0.00031**
PC/PS	**0.00456**		0.04026
PC/SM	**0.00031**	0.04026	

Slow k_{on}

	PC only	PC/PS	PC/SM
PC only		0.30943	**0.00107**
PC/PS	0.30943		**0.00003**
PC/SM	**0.00107**	**0.00003**	

.

Supplementary Table S2. P values for PMT-N binding to natural membranes. Shown are P values calculated with the t-distribution for comparing PMT-N binding characteristics on natural and enzyme-treated membranes. The degree of freedom used for *p* value calculation was based on the number of sets (N) with four traces for Rapid B_{max} and Rapid K_D, and the total number of traces (N x 4) for others.

Rapid B_{max}

	Native	Trypsin	SMase	SMase/T	PLDCab	PLDCab/T	PLDSc
Native		**0. 00019**	**0. 01070**	**0. 00006**	**0. 00530**	**0. 00442**	**0. 00075**
Trypsin	**0. 00019**		**0. 00972**	**0. 00005**	**0. 00007**	**0. 00662**	**0. 00174**
SMase	**0. 01070**	**0. 00972**		0. 06867	**0. 01022**	**0. 01020**	**0. 00999**
SMase/T	**0. 00006**	**0. 00005**	0. 06867		**0. 00005**	**0. 00005**	**0. 00005**
PLDCab	**0. 00530**	**0. 00007**	**0. 01022**	**0. 00005**		0. 12500	0. 00200
PLDCab/T	**0. 00442**	**0. 00662**	**0. 01020**	**0. 00005**	0. 12500		0. 00243
PLDSc	**0. 00075**	**0. 00174**	**0. 00999**	**0. 00005**	0. 00200	0. 00243	

Rapid K_D

	Native	Trypsin	SMase	SMase/T	PLDCab	PLDCab/T	PLDSc
Native		0. 00047	0. 02782	**0. 00000**	0. 04590	0. 01425	**0. 00102**
Trypsin	**0. 00047**		0. 01799	**0. 00014**	**0. 00033**	0. 01999	0. 00268
SMase	0. 02782	0. 01799		0. 06950	0. 02664	0. 02215	0. 02059
SMase/T	**0. 00000**	**0. 00014**	0. 06950		**0. 00026**	**0. 00020**	**0. 00018**
PLDCab	0. 04590	**0. 00033**	0. 02664	**0. 00026**		**0. 00248**	**0. 00010**
PLDCab/T	0. 01425	0. 01999	0. 02215	**0. 00020**	**0. 00248**		**0. 01210**
PLDSc	**0. 00102**	0. 00268	0. 02059	**0. 00018**	**0. 00010**	**0. 01210**	

Rapid k_{off}

	Native	Trypsin	SMase	SMase/T	PLDCab	PLDCab/T	PLDSc
Native		0. 60945	**0. 00248**	**0. 00015**	**0. 00000**	**0. 00000**	**0. 00043**
Trypsin	0. 60945		**0. 00304**	**0. 00021**	**0. 00000**	**0. 00000**	**0. 00069**
SMase	**0. 00248**	**0. 00304**		0. 55732	0. 29540	0. 08958	0. 15497
SMase/T	**0. 00015**	**0. 00021**	0. 55732		0. 55985	0. 09566	0. 25926
PLDCab	**0. 00000**	**0. 00000**	0. 29540	0. 55985		0. 08714	0. 43617
PLDCab/T	**0. 00000**	**0. 00000**	0. 08958	0. 09566	0. 08714		0. 71455
PLDSc	**0. 00043**	**0. 00069**	0. 15497	0. 25926	0. 43617	0. 71455	

Supplementary Table S2 (continued).

Slow B_{max}

	Native	Trypsin	SMase	SMase/T	PLDCab	PLDCab/T	PLDSc
Native		**0. 00031**	**0. 00007**	**0. 00176**	**0. 00000**	**0. 00009**	0. 00003
Trypsin	**0. 00031**		0. 19828	0. 08791	**0. 00013**	0. 30842	0. 03425
SMase	**0. 00007**	0. 19828		0. 01840	0. 01607	0. 48796	0. 00113
SMase/T	**0. 00176**	0. 08791	0. 01840		**0. 00000**	**0. 00387**	0. 00012
PLDCab	**0. 00000**	**0. 00013**	0. 01607	**0. 00000**		**0. 00031**	0. 00318
PLDCab/T	**0. 00009**	0. 30842	0. 48796	**0. 00387**	**0. 00031**		0. 13384
PLDSc	0. 00003	0. 03425	0. 00113	0. 00012	0. 00318	0. 13384	

Slow K_D

	Native	Trypsin	SMase	SMase/T	PLDCab	PLDCab/T	PLDSc
Native		0. 23276	**0. 01239**	**0. 00132**	0. 05050	0. 23865	1. 00000
Trypsin	0. 23276		**0. 00760**	**0. 00067**	**0. 00707**	0. 02907	0. 09302
SMase	**0. 01239**	**0. 00760**		0. 67319	0. 04130	0. 02220	0. 01095
SMase/T	**0. 00132**	**0. 00067**	0. 67319		0. 04849	0. 02232	0. 01158
PLDCab	0. 05050	**0. 00707**	0. 04130	0. 04849		0. 30814	0. 03688
PLDCab/T	0. 23865	0. 02907	0. 02220	0. 02232	0. 30814		0. 11431
PLDSc	1. 00000	0. 09302	0. 01095	0. 01158	0. 03688	0. 11431	

Slow k_{off}

	Native	Trypsin	SMase	SMase/T	PLDCab	PLDCab/T	PLDSc
Native		0. 02887	0. 59045	0. 38651	**0. 00000**	**0. 00024**	0. 17290
Trypsin	0. 02887		0. 20330	0. 03413	**0. 00011**	**0. 00658**	0. 77319
SMase	0. 59045	0. 20330		1. 00000	**0. 00520**	0. 03305	0. 25943
SMase/T	0. 38651	0. 03413	1. 00000		**0. 00002**	**0. 00091**	0. 07725
PLDCab	**0. 00000**	**0. 00011**	**0. 00520**	**0. 00002**		0. 03169	**0. 00022**
PLDCab/T	**0. 00024**	**0. 00658**	0. 03305	**0. 00091**	0. 03169		0. 01450
PLDSc	0. 01536	0. 25351	0. 11539	0. 01353	**0. 00146**	0. 11810	

Slow k_{on}

	Native	Trypsin	SMase	SMase/T	PLDCab	PLDCab/T	PLDSc
Native		0. 08768	**0. 00000**	**0. 00000**	0. 40862	0. 23865	0. 30252
Trypsin	0. 08768		**0. 00000**	**0. 00000**	0. 52789	0. 61625	0. 38466
SMase	**0. 00000**	**0. 00000**		**0. 06419**	**0. 00000**	**0. 00035**	**0. 00000**
SMase/T	**0. 00000**	**0. 00000**	**0. 06419**		**0. 00001**	**0. 00050**	**0. 00000**
PLDCab	0. 40862	0. 52789	**0. 00000**	**0. 00001**		1. 00000	1. 00000
PLDCab/T	0. 23865	0. 61625	**0. 00035**	**0. 00050**	1. 00000		1. 00000
PLDSc	0. 30252	0. 38466	**0. 00000**	**0. 00000**	1. 00000	1. 00000	

Supplementary Table S3. Receptors of selected protein toxins.

Toxins	Lipid/Glycolipid Receptor	Protein Receptor
CT	GM_1 [1]	
DT		HB-EGF [2]
PT	NeuAcα(2,6)-Gal [3], GD_{1a} [4]	
α-Toxin	Phosphatidylcholine [5]	
δ-Toxin	GM_2 [6]	
C2 Toxin	N-linked carbohydrates [7]	
CNF1	HSPG [8]	LRP [9]
PMT	SM, PC, LacCer [this study]	
AnTx		CMG2 [10]
BoNT/A	GD_{1a}, GT_{1b}, GD_{1b} [11]	SV2 [12]
BoNT/B	GD_{1a}, GT_{1b}, [11, 13]	Syt I, Syt II [14]
BoNT/C	GD_{1a}, GT_{1b}, GD_{1b} [11, 15]	
BoNT/D	GD_{1a}, GT_{1b}, GD_{1b} [11], [16]	
BoNT/E	GD_{1a}, GT_{1b}, GD_{1b} [11]	SV2 [11]
BoNT/F	GD_{1a}, GT_{1b} [11, 17]	SV2[11, 17]
BoNT/G	GT_{1b} [18]	Syt I, Syt II [14, 18]
ETA		$α_2$MR/LRP [19]
STx	Gb3, Gb4 [20]	
TeNT	GT_{1b} [21]	
Tcd	Galβ1-4GlcNac [22]	
VacA	SM [23]	

Abbreviations: α-Toxin, *Clostridium perfringens* α-toxin; AnTx, anthrax toxin; BoNT/A *C. botulinum* neurotoxins; C2 Toxin, C. *botulinum* C2 toxin; CNF1, cytotoxic necrotizing factor 1; CT, cholera toxin; Delta toxin, C. *perfringens* delta toxin; DT, diphtheria toxin; PT, pertussis toxin; STx, Shiga toxin; Tcd, *C. dificile* toxins; TeNT, tetanus toxin; VacA, *H. pylori* toxin VacA; ETA, *Pseudomonas aeruginosa* exotoxin A; SM, sphingomyelin; GM, monosialotetrahexosylganglioside; Gb, globotriosylceramide; CMG2, human capillary morphogenesis protein 2; SV2, synaptic vesicle protein 2; LRP, laminin receptor precursor; $α_2$-MR/LRP, $α_2$-macroglobulin receptor/low density lipoprotein receptor-related protein; HB-EGF, heparin-binding EGF-like growth factor.

References:

1. Cumar, F.A., B. Maggio, and R. Caputto, *Ganglioside-Cholera Toxin Interactions - a Binding and Lipid Monolayer Study.* Molecular and Cellular Biochemistry, 1982. **46**(3): p. 155-160.
2. Naglich, J.G., et al., *Expression Cloning of a Diphtheria-Toxin Receptor - Identity with a Heparin-Binding Egf-Like Growth-Factor Precursor.* Cell, 1992. **69**(6): p. 1051-1061.
3. Stein, P.E., et al., *Structure of a Pertussis Toxin Sugar Complex as a Model for Receptor-Binding.* Nature Structural Biology, 1994. **1**(9): p. 591-596.
4. Janshoff, A., et al., *Quartz crystal microbalance investigation of the interaction of bacterial toxins with ganglioside containing solid supported membranes.* Eur Biophys J, 1997. **26**(3): p. 261-70.
5. Jepson, M., et al., *Differences in the carboxy-terminal (putative phospholipid binding) domains of Clostridium perfringens and Clostridium bifermentans phospholipases C influence the hemolytic and lethal properties of these enzymes.* Infection and Immunity, 1999. **67**(7): p. 3297-3301.
6. Jolivetreynaud, C., B. Hauttecoeur, and J.E. Alouf, *Interaction of Clostridium-Perfringens-Delta-Toxin with Erythrocyte and Liposome Membranes and Relation with the Specific Binding to the Ganglioside Gm2.* Toxicon, 1989. **27**(10): p. 1113-1126.
7. Eckhardt, M., et al., *Binding of Clostridium botulinum C2 toxin to asparagine-linked complex and hybrid carbohydrates.* Journal of Biological Chemistry, 2000. **275**(4): p. 2328-2334.
8. Blumenthal, B., et al., *The cytotoxic necrotizing factors from Yersinia pseudotuberculosis and from Escherichia coli bind to different cellular receptors but take the same route to the cytosol.* Infection and Immunity, 2007. **75**(7): p. 3344-3353.
9. Chung, J.W., et al., *37-kDa laminin receptor precursor modulates cytotoxic necrotizing factor 1-mediated RhoA activation and bacterial uptake.* Journal of Biological Chemistry, 2003. **278**(19): p. 16857-16862.
10. Scobie, H.M., et al., *Human capillary morphogenesis protein 2 functions as an anthrax toxin receptor.* Proceedings of the National Academy of Sciences of the United States of America, 2003. **100**(9): p. 5170-5174.
11. Rummel, A., et al., *Botulinum neurotoxins C, E and F bind gangliosides via a conserved binding site prior to stimulation-dependent uptake with botulinum neurotoxin F utilising the three isoforms of SV2 as second receptor.* Journal of Neurochemistry, 2009. **110**(6): p. 1942-1954.
12. Dong, M., et al., *SV2 is the protein receptor for botulinum neurotoxin A.* Science, 2006. **312**(5773): p. 592-596.
13. Nishiki, T., et al., *The high-affinity binding of Clostridium botulinum type B neurotoxin to synaptotagmin II associated with gangliosides G(T1b)/G(D1a).* Febs Letters, 1996. **378**(3): p. 253-257.
14. Dong, M., et al., *Synaptotagmins I and II mediate entry of botulinum neurotoxin B into cells.* J Cell Biol, 2003. **162**(7): p. 1293-303.
15. Tsukamoto, K., et al., *Binding of Clostridium botulinum type C and D neurotoxins to ganglioside and phospholipid - Novel insights into the receptor for clostridial neurotoxins.* Journal of Biological Chemistry, 2005. **280**(42): p. 35164-35171.

16. Strotmeier, J., et al., *Botulinum neurotoxin serotype D attacks neurons via two carbohydrate-binding sites in a ganglioside-dependent manner.* Biochem J, 2010. **431**(2): p. 207-16.
17. Fu, Z.J., et al., *Glycosylated SV2 and Gangliosides as Dual Receptors for Botulinum Neurotoxin Serotype F.* Biochemistry, 2009. **48**(24): p. 5631-5641.
18. Schmitt, J., et al., *Structural Analysis of Botulinum Neurotoxin Type G Receptor Binding.* Biochemistry, 2010. **49**(25): p. 5200-5205.
19. Kounnas, M.Z., W.S. Argraves, and D.K. Strickland, *The 39-Kda Receptor-Associated Protein Interacts with 2 Members of the Low-Density-Lipoprotein Receptor Family, Alpha-2-Macroglobulin Receptor and Glycoprotein-330.* Journal of Biological Chemistry, 1992. **267**(29): p. 21162-21166.
20. Keusch, G.T., M. Jacewicz, and A. Donohuerolfe, *Pathogenesis of Shigella Diarrhea - Evidence for an N-Linked Glycoprotein Shigella Toxin Receptor and Receptor Modulation by Beta-Galactosidase.* Journal of Infectious Diseases, 1986. **153**(2): p. 238-248.
21. Herreros, J., T. Ng, and G. Schiavo, *Lipid rafts act as specialized domains for tetanus toxin binding and internalization into neurons.* Molecular Biology of the Cell, 2001. **12**(10): p. 2947-2960.
22. Voth, D.E. and J.D. Ballard, *Clostridium difficile toxins: Mechanism of action and role in disease.* Clinical Microbiology Reviews, 2005. **18**(2): p. 247-+.
23. Gupta, V.R., et al., *Sphingomyelin functions as a novel receptor for Helicobacter pylori VacA.* Plos Pathogens, 2008. **4**(5): p. -.